axis perpendicular to the arch plane. In order to prevent slipping and to give full play to an arch action, the ends of the arches were carefully fixed against horizontal displacements. Since it is difficult to realize a distributed radial load, group of vertical concentrated loads was applied in place of it. The loading devices are shown in Photo 1. The piano wire were used as to follow the displacement outward the arch plane without restraint, but the excentricity of loading was inevitable because of the cross-sectional shape of model arch. The loading rod was pulled downward by a hydraulic jack. Model arch was loaded gardually and carefully not to produce disturbance.

	Theoretical values			Experimental values		$\frac{\overline{P}_E}{P_T}\times 100$ (%)
	λ_T	P_{cr} (kg/cm)	$P_T=2P_{cr}L$ (kg)	P_E (kg)	$\overline{P}_E=P_E\left(\frac{\theta_0}{\sin\theta_0}\right)^{17)}$ (kg)	
Model arch	40.0	7.9	1754	1400	1555	88.6
Single arch	32.25	6.29	1398	——	——	——

Table 2 Theoretical and experimental buckling load

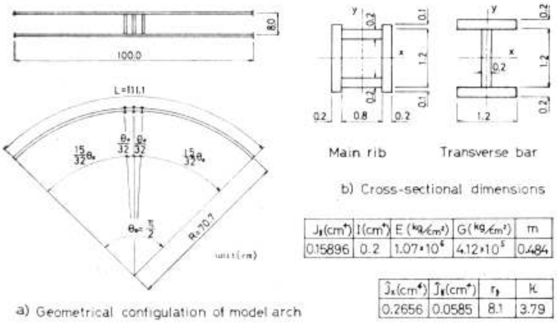

a) Geometrical configulation of model arch

b) Cross-sectional dimensions

J_θ (cm⁴)	I (cm⁴)	E (kg/cm²)	G (kg/cm²)	m
0.15896	0.2	1.07×10^6	4.12×10^5	0.484

$\hat{J}_x$ (cm⁴)	$\hat{J}_y$ (cm⁴)	r_y	K
0.2656	0.0585	8.1	3.79

Fig. 10 Model arch

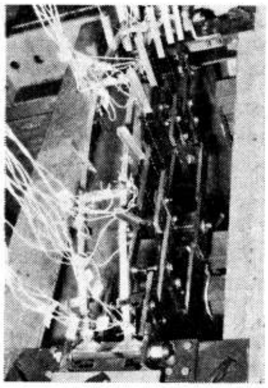

Photo 1 Loading devices

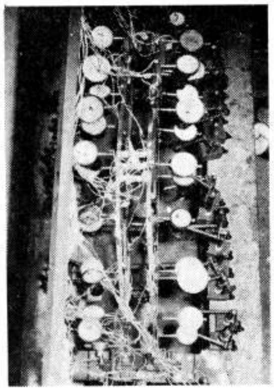

Photo 2 Critical equilibrium state at $P=1.35$ ton

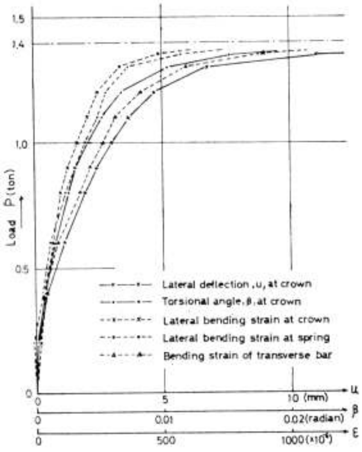

Fig. 11 Load vs. deformation curves

(3) Results and Consideration

The ultimate load was estimated as $P=1.40$ t from the asymptote of the load-deformation curves. The model arch in critical equilibrium state at $P=1.35$ t is shown in Photo 2. Test results are illustrated in Fig. 11. These curves show the effects of initial imperfection in lower range of loading, but to avoid them was, actually, difficult. Both the buckling load obtained from the theoretical analysis and model test are shown in Table 2. The experimental value shows about 90%-coincidence with the theoretical one.

4. CONCLUSIONS

The following conclusions will be drawn within the scope of the given assumptions and idealizations :

1) Transfer matrix method was employed effectively in obtaining the eigenvalue of the differential equation governing the buckling of complicated structures which consist of main systems and branch systems.

2) Results of numerical computation about several arches are illustrated as the curves of buckling coefficient versus flexural rigidity of the transverse bars.

3) The arrangement of the transverse bars are in close relation to the shape of buckling mode of corresponding single arch. To arrange the transverse bars of large flexural rigidity at the location where corresponding large deformations of the arched ribs occurs is effective from the view point of lateral stability. That may be, in other words, to increase the total strain energy stored in the transverse bars during the buckling deformation.

4) In order to interprete the relation between the cross-sectional quantities of the arched rib and the effects of transverse bars, the ratio, γ, of the maximum value of the torsional angle, $\beta_{\max}$, to that of lateral deflection angle, $\alpha_{\max}'$ are quite